Title
D2O PRODUCT ANGULAR AND TRANSLATIONAL ENERGY DISTRIBUTIONS FROM THE OXIDATION OF DEUTERIUM ON Pt(lll)

Permalink
https://escholarship.org/uc/item/0gh8d3sp

Author
Ceyer, S.T.

Publication Date
1982-12-01

LBL-15035 c2
Preprint

Lawrence Berkeley Laboratory
UNIVERSITY OF CALIFORNIA

Materials & Molecular Research Division

Submitted to the Journal of Chemical Physics

D_2O PRODUCT ANGULAR AND TRANSLATIONAL ENERGY DISTRIBUTIONS FROM THE OXIDATION OF DEUTERIUM ON Pt(111)

S.T. Ceyer, W.L. Guthrie, T.-H. Lin, and
G.A. Somorjai

December 1982

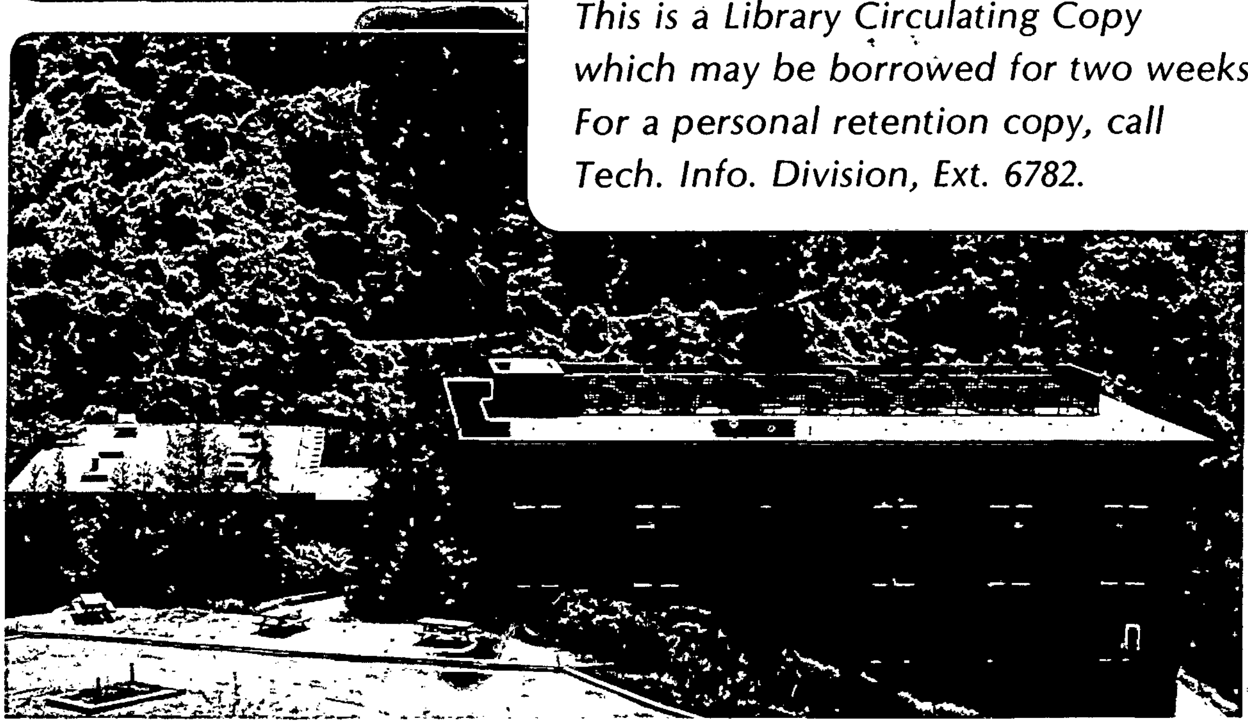

Prepared for the U.S. Department of Energy under Contract DE-AC03-76SF00098

D_2O Product Angular and Translational Energy Distributions from the Oxidation of Deuterium on Pt(111)

S. T. Ceyer*, W. L. Guthrie, T.-H. Lin, and G. A. Somorjai

Materials and Molecular Research Division, Lawrence Berkeley Laboratory
and
Department of Chemistry, University of California, Berkeley, CA 94720

Abstract

The angular and translational energy distribution of D_2O produced from the oxidation of deuterium on the (111) crystal face of platinum have been measured in the surface temperature range of T_s = 664K - 913K. Although the angular distribution can be described by a cosine function, the translational energy distributions deviate substantially from the corresponding Maxwell-Boltzmann distributions. The D_2O mean translational energy, <E>/2k, varies from 260K to 460K over the temperature range investigated. Two mechanisms for the production of translationally cold product molecules are discussed.

....

* Permanent Address: Department of Chemistry
Massachusetts Institute of Technology
Cambridge, MA 02139

This work was supported by the Director, Office of Energy Research, Office of Basic Energy Sciences, Materials Science Division of the U.S. Department of Energy under Contract DE-AC03-76SF00098, and the National Science Foundation.

Introduction

The dynamics of the last bond formation step or the desorption step determine the spatial and translational energy distributions of the products from a surface chemical reaction. Measurement of these distributions in a molecular beam reactive scattering experiment thus provides information on the mechanism and dynamics of the exit process. For example, they can provide a means of determining the concertedness of the final step of the reaction and the desorption process, the amount of the exoergicity channeled into translation, the relative rates of thermal excitation of an adsorbate to desorption, or the shape of the potential energy surface in the exit channel region. The translational energy distribution measurements of H_2 produced from the recombination of $H_{(a)} + H_{(a)}$ on polycrystalline nickel [1,2], Ni(111) [3], Pd(100) [4], and of CO_2 produced from the reaction of CO + O_2 on polycrystalline platinum [5] are examples of the determination of the shape of the potential energy surface. The large translational energies observed result from the presence of a barrier in the exit channel which, in the case of CO_2, may be related to the formation of a bent O=C=O bond [6-8] in the transition state. The peaking of the H_2 and CO_2 angular distributions at the surface normal is due to the parallel orientation of the barrier equipotentials which causes focusing of the product molecules towards the normal.

To date, this is the only type of dynamics that has been observed and the only reactive systems that have been studied. The fact that the exit barrier is very effectively channeled into translation indicates that the rate of energy dissipation into the surface is slow relative to the velocity of the newly formed molecule. Thus, it is reasonable that systems can be found where the exoergicity of the last bond formation step is effectively channeled into translation. However, if the exoergicity of the reaction is small or nonexistent, then the newly formed product molecule has a greater probability of becoming trapped on the surface thereby uncoupling the final reaction step and desorption step. A product angular distribution described by a cosine function and a product translational energy distribution characterized by a Maxwell-Boltzmann function at the temperature of the surface is a signature for this type of dynamics.

At first glance the reaction $D_2 + O_2 \rightarrow D_2O$ on Pt(111) might be cited as an example of this latter mechanism. The D_2O product angular distribution has been observed to fit a cosine function [9]. By conventional interpretations this implies that the translational energy should be in equilibrium with the solid. We have expanded on this previous study to include energy distribution measurements as a function of surface temperature and scattering angle. We report here both the angular and energy distributions of D_2O produced in this reaction. Our angular distribution measurements agree with the earlier measurements. However, the translational energy distributions indicate that the conventional interpretation must be modified.

Experimental

The apparatus was constructed to study energy partitioning in surface chemical reactions [8,10]. A schematic of it is shown in Fig. 1. The reactants, D_2 and O_2, were each expanded from a 0.08 mm diameter supersonic nozzle at a stagnation pressure of 200 Torr. The D atom beam was produced from a microwave discharge source, previously described in detail [10]. The twice differentially pumped beams intersect at an angle of 30° at the crystal surface. The angle of incidence is 49°. The product flux is mass analyzed and detected by a twice differentially pumped quadrupole mass spectrometer. The detector is rotatable about the single crystal sample allowing measurement of product angular distributions and velocity distributions at each angle. A tuning fork chopper at 150 Hz modulated one of the incident beams during the angular distribution measurements. A cross correlation time-of-flight technique [11] was used for the velocity distribution measurements. The product flux was modulated in these measurements.

The Pt(111) sample was cleaned by argon ion sputtering, and when needed by chemical cleaning in oxygen at a surface temperature of 700K. Surface cleanliness was determined by Auger electron spectroscopy (AES). The crystal was annealed at 1100K and then lowered to the reaction temperature. The crystal temperature was determined by a Pt - Pt 10% Rh thermocouple. After each hour of data collection, the crystal surface cleanliness was checked by AES. There was always oxygen contamination on the order of 10-20% of a monolayer regardless of the temperature at which the reaction occurred. Coverage was based on a calibration by Gland [12].

The D_2O signal count rates were typically 30 - 80 ions/s against a background count rate at m/e = 20 of 7000 ions/s. With the low count rates, approximately 20 hours of real data collection time was required for each distribution and approximately 2 to 3 times that in actual experimental time.

The low product count rates and the pronouncedly slow TOF distributions caused some concern that spurious sources of signal might be affecting the distributions. Since the resolution of the mass spectrometer was decreased in order to increase transmission, we measured a TOF distribution with no D_2 incident on the surface in order to determine if incomplete filtering of the O^+ (m/e = 16) ionization fragment from the scattered O_2 was occurring. After 3 hours, no distribution was observed with the mass filter tuned to m/e = 20. It was determined that the O^+ fragment contributed at most 0.5 ions/s to the signal. Inelastic scattering of background D_2O from the crystal into the detector is another possible spurious source of signal. The background D_2O is produced from the reaction of D_2 and O_2 on filaments, chamber surfaces, and in the ion pump. Blank experiments with both beams entering the scattering chamber, but only one incident on the crystal, showed that the effect of background D_2O is negligible.

The time of flight spectrum was calibrated against the flight times for a series of four inert gases from an effusive source at 300K and against the flight time of D_2O from an effusive source at two temperatures. The effusive source was a 0.08 mm diameter hole in an oven operated at a stagnation pressure of $8x10^{-2}$ Torr. Fig. 2 shows the TOF distributions observed for a source temperature of 310K and 655K. The solid curves represent Maxwell-Boltzmann distributions at the source temperature, convoluted with the known chopper gate and electronic gate functions. As can be seen, the experimental distributions agree with the expected Maxwell-Boltzmann distributions.

Results

Fig. 3a shows the angular distribution observed for product D_2O taken from the reaction $D_2 + O_2$ at a surface temperature T_s=700K. Fig. 3b shows the product D_2O angular distribution from the reaction $D + O_2$ at the same temperature. Within the uncertainty, the angular distributions resulting from the atomic or molecular deuterium reactants are identical. As discussed below, depending on the desorption mechanism, this similarity may indicate that D atoms rather than D_2 are essential intermediates in this reaction. Plotted with the data is a cosine function (solid line), showing that the number density is proportional to the cosine of the desorption angle, as reported previously by Smith and Palmer [9]. By micro-reversibility arguments, cosine angular distributions are commonly taken to imply equilibration of the desorbing gas with the surface [13]. However, the TOF distributions are far from equilibrium.

The time-of-flight distribtions, transformed to energy distributions, are shown in Figs. 4 and 5. The collected TOF distributions are number density distributions, $P_d(t)$, and are multiplied by the velocity to transform to flux distributions, $P_f(t)$. The transformation to an energy distribution is made by multiplication by the Jacobian so that $P(E) \propto t^3 P_f(t) \propto t^2 P_d(t)$. The data for surface temperatures of 913K, 870K and 765K are shown in Figs. 4a, 4b and 4c. Two distributions for T_s = 664K at detector angles $\Theta = 7°$ and 40° from the surface normal are shown in Fig. 5. Plotted as the open circles is a Maxwell-Boltzmann distribution at the corresponding surface temperature, convoluted with the chopper and electronic gating function and normalized to the total counts of the experimental distribution. The striking feature of these distributions is that they lack the high energy tail of the corresponding Maxwell-Boltzmann distributions.

The mean energies in terms of equivalent temperature, $\langle E\rangle/2k$, the statistical errors of the mean energies, and the relative distribution widths $\langle v^2 - \langle v\rangle^2\rangle/\langle v\rangle^2$, are tabulated in Table I. The relative widths are all significantly smaller than the value for a Maxwell-Boltzmann distribution, 0.132.

The relative D_2O production rates at the five temperatures examined in this study are shown in Fig. 6a. The D_2O production rate as a function of the O_2 source stagnation pressure is shown in Fig. 6b. The production rate is approximately linear with O_2 intensity. The production rate is nearly independent of D_2 intensity and was essentially unchanged when the D_2 source stagnation pressure was reduced from 200 Torr to 100 Torr. The H_2 sticking coefficient for dissociative adsorption has been measured to be approximately 0.10 on Pt(111) [14-16]. A wide range of values has been reported for the O_2

dissociative adsorption probability [12, 17-21] which appears to fall exponentially with decreasing defect density and with increasing oxygen coverage [12, 17-19]. In this study, it appears that the O_2 dissociative adsorption probability is limiting the rate.

Discussion

The observation that the mean energy of product molecules from a surface chemical reaction is substationally less than the mean energy of the solid at some temperature is unusual. Previous measurements of translational energy distributions of product molecules have shown that the mean energy is substantially larger than the mean energy of the solid. This was the case for H atom recombination on Ni and Pd [1-4] and for the oxidation of CO on Pt [5].

It is necessary to review the energetics of the adsorption of D_2, O_2, OD and D_2O on Pt(111) in order to discuss the possible mechanisms for the production of unequilibrated and cold distributions. An energy level diagram is shown in Figure 7. The overall reaction $D_{2(g)} + O_{2(g)} \rightarrow D_2O_{(g)} + O_{(a)}$ is exothermic by 83 kcal/mole. Much of this energy is not available to translation of the molecule away from the surface but is released and dissipated into the solid during the dissociative adsorption of the reactants. The dissociative adsorption of D_2 and O_2 on Pt(111) liberates 15 kcal/mole [15, 16, 22] and 50 kcal/mole [12, 23], respectively. There is also a weaker dissociative state of hydrogen on Pt(111) at high coverages [16] with a heat of adsorption of 5 kcal/mole. In addition to these states, evidence [15] for an H_2 molecular precursor state with a heat of adsorption of much less than 5 kcal/mole and an O_2 molecular precursor state with a heat of adsorption of 8 kcal/mole [12, 23] has been cited. However, since the surface temperatures at which this reaction was carried out are high, only the deeper dissociative states of D_2 and O_2 are significantly populated. Additional support for the dissociative state of D_2 comes from the fact that the D_2O angular distributions are identical whether the starting reactant is D_2 or D. Now, if the three adsorbed atomic species, 2D and O, shown in Fig. 7 simultaneously collided and then desorbed immediately following their reaction forming D_2O, 18 kcal of energy would be available to translational energy. However, a two-body collision forming an OD species followed by a second collision between OD and D or between two OD species is more likely to occur than a three-body collision. This two-step mechanism requires the presence of stable OH radicals on the surface. Recently OH radicals on the Pt(111) surface have indeed been observed [24] and Lin and coworkers have observed desorption of OH radicals during the water production reaction on an uncharacterized polycrystalline Pt surface. They measured the apparent activation energy for OH appearance in the gas phase to be 31 kcal/mole [25]. In the two step mechanism the amount of energy available to translation is then dictated by the exoergicity of the second step, $OD_{(a)} + D_{(a)} \rightarrow D_2O_{(g)}$. Since the bond energies of D-Pt and of D_2O are known, the amount of energy believed to be available for translation depends acutely on knowledge of the binding energy of the OD radical. If the apparent activation energy quoted above represents the OH desorption energy from a clean platinum single crystal surface, then the exoergicity of the reaction, or the total energy available to translation is about 30 kcal/mole for the OD + D reaction and 39 kcal/mole for the $OD_{(a)} + OD_{(a)} \rightarrow D_2O_{(g)} + O_{(a)}$ reaction. However, with this OH energy one finds that OH formation should be energetically unfavorable (Fig. 7), in contradiction to the observation of OH radicals on Pt surfaces [24, 25]. Since the binding energy of water in the above mentioned experiment [25] was measured to be 14 kcal/mole less than that measured for water on Pt(111) using different techniques [26], we assume that as a consequence the binding energy of the OD radical on the platinum surface is also larger by approximately 14 kcal/mole. Then the total energy available to translation is 17 kcal/mole for the OD + D reaction and 9 kcal/mole for the OD + OD reaction. The uncertainty in the energetics involving the OD intermediate is shown in Figure 7.

It is clear that the chemical energy released is not predominantly transferred into translation of the molecule away from the surface. The average energies of the measured distributions are hardly a tenth of the cited exoergicities. It might be suggested that the OH binding energy is actually larger than the values discussed above, such that the final bond formation step has really very little or no excess energy. However, a final reaction step with a small exoergicity cannot explain these velocity distributions. Kinetic measurements have shown that reaction times are long: 63 μs at 850K to 1 ms at 600K [9]. Since these times are long, the intermediates attain equilibrium with the surface and thus, the energy of the D_2O molecule should be at least that which would correspond to the equilibrium state of the reactants $OD_{(a)}$ and $D_{(a)}$. Consider, however, a mechanism in which the bond formation step and the desorption process are not concerted. That is, once the D_2O molecule is formed, it remains on the surface for many vibrational periods, dissipating the energy released in the bond formation step to the surface and thereby attaining equilibrium with the surface. Fig. 8 represents such an ensemble of equilibrated D_2O molecules. The solid curve is the Boltzmann function for a temperature of 870K and it is shown relative to a representation of the 15 kcal/mole D_2O-Pt potential energy well [26] (dashed curve). As can be seen most of the ensemble lies below the edge of the well. Approximating the density of vibrational levels by the density of levels for a harmonic oscillator and integrating for the well depth, one finds that more than 99% of the initial ensemble is below the edge of the well.

As indicated in Fig. 8, the rate of desorption increases with increasing energy and is proportional to the normal component of the velocity v_z, i.e. $v \cos\theta$. The probability of observing a given translational energy in the gas phase is proportional to the desorption rate, the probability of populating an energy level above the edge of the well and the density of states. For adsorbed molecules whose energies are characterized by a Boltzmann distribution the translational energy distributionn of the flux upon desorption is given by the Maxwell-Boltzmann distribution $v^3\exp(-mv^2/2kT)$, and the angular distribution of the flux is given by $\cos\theta$ where θ is measured from the surface normal [27]. These distributions hold, however, only if the rate of thermal excitation of the adsorbed molecules by the solid is fast relative to the desorption rate [27-29]. If the desorption rate is fast relative to the excitation rate, then the desorption process depletes molecules from the upper energy levels thereby perturbing the energy distribution away from equilibrium [30]. The result is that the observed velocity distribution is slower than what would be expected from prior equilibration of the adsorbed molecule with the surface [28, 29, 31]. Our observations are not out of line with this mechanism. Early studies of gas phase reactions indicated that non-equilibrium effects should become important when the ratio of the activation energy to temperature, E_a/kT, is less than 5-10 [32-34]. In our case, E_a/kT ranges from 17 to 9, the upper limit set by those studies. Strong non-equilibrium effects were predicted for Xe and Ar desorption from Pt(111) for $E_a/kT=10$, and that these effects persist for somewhat larger ratios [29, 31].

Since energy in the z direction leads to desorption, the amount of energy that can be transferred in that direction is limited. Since motion in the x-y direction does not lead to desorption, there should be a higher average velocity component parallel to the surface than perpendicular to it. This has two consequences: the angular distribution will be slightly broader than cosine and the mean velocities will be higher as the desorption angle increases [31]. A nearly cosine angular distribution was found for calculations of Ar and Xe desorption from Pt(111) [29]. If coupling between the parallel and perpendicular motion is strong, then the angular distribution should become more similar to a cosine function and the mean velocities more angle independent. The motion of the structurally complex and more strongly bound D_2O molecule should exhibit more efficient coupling than Ar or Xe, so that the cosine angular distribution and apparent angular independence of the velocity (Fig. 5) are not inconsistent with non-equilibrium desorption.

This mechanism for desorption predicts that the mean translational energy dependence on surface temperature should be linear at low surface temperatures. As the surface temperature is increased, the mean translational energy will gradually deviate from the equilibrium value to lower energies and finally arrive at some asymptotic value. This behaviour was observed in an early study of the mean energies of a variety of molecules scattered from a graphite surface [35]. The mean energies were independent of incident beam energy which indicated that the molecules were indeed trapped and that what was being observed was non-equilibrium desorption. Since the rate of the production of D_2O decreases drastically at low T_s, it is impossible to carry out the TOF measurements at low T_s. Thus, it is reasonable that this linear region is not observed in Table I. In the intermediate range of T_s, the mean values of the D_2O translational energies have a weak positive dependence on surface temperature as shown in Fig. 9. However, instead of reaching an asymptotic value they increase again somewhat at higher temperatures. This is an interesting observation. If non-equilibrium desorption is occurring, then the interaction between D_2O and the surface must have become more attractive at the higher surface temperature, 913K. This could be a result of a change in coverage of reactants whose presence modifies the interaction between D_2O and the Pt surface. Oxygen is the more likely of the reactants to be the cause of this shift since the recombination-desorption temperature of O_2 on Pt(111) occurs between 850-900K, depending on coverage. However, there was no correlation between the amount of oxygen remaining on the surface after the reaction and the surfce temperature. There was always an oxygen coverage of 10-20% of a monolayer after the reaction. The temperature stability of this adsorbed oxygen indicates that it is probably in an oxide form [23]. There remains the question as to whether the steady state concentration of chemisorbed oxygen has changed at the highest temperature studied. This is likely because the rate of the reaction also levels off here, presumably because of recombination and desorption of O_2 or of the desorption of the OH radical. However, the effect of the chemisorbed oxygen coverage on the D_2O-Pt binding energy is unknown.

The data reported here is consistent with non-equilibrium desorption, but with some unresolved points in the interpretation, so a mechanism incorporating concerted formation and desorption will be considered. Such mechanisms have been discussed in the literature for systems in which an exit channel potential energy barrier exists, the excess potential energy then converted into translational energy [1-7]. Some circumstances that might produce cold, unequilibrated product molecules are proposed.

As discussed above, it is likely that the reaction proceeds through the formation of an OD intermediate. The D-OD distance is then the primary reaction coordinate for the final step of the reaction. Since the potential energy surface is multi-dimensionsal the potential energy of that coordinate is also likely to be a function of the Pt-OD distance. For example, a sharp minimum in the DO-D barrier height as a function of Pt-OD seperation would restrict the reaction to occur at a given surface bond distance. If this distance is large it is likely that the half of the newly formed molecules with velocities directed away from the surface can desorb without further energy exchange with the surface. The molecules with velocities toward the surface may experience additional energy transfer that will tend to smear out the nascent energy distribution.

The translational energy distribution will then depend on whether the final step is exoergic, the distributions of energy in the reactants prior to the final reaction step, conservation of momentum for the reactants, and the effects of any forces that may be exerted by the surface during the D_2O formation. For long surface residence times, it is likely that the distribution of energies for the reactants will be Boltzmann at the temperature of the surface.

It seems likely that the above considerations for a non-exergic final step could lead to product translational energy distribrtions that are not in equilibrium with the surface. However, it is beyond the scope of this paper to determine if these considerations can account for translational energies as low as those observed.

The D_2O translational energy distributions (Figs. 4 and 5) and angular diatributions (Fig. 3) demonstrate that a cosine angular distribrtion can result even if thermal equilibrium is not attained. The common association of a cosine angular distribution with equilibrium between the gas and the surface is not always correct. The flux of molecules desorbing from the surface will always exhibit a cosine dependence on angle from the surface normal if the velocity is isotropic and the rate of appearance in the gas phase is v_z dependent. It is unnecessary for the velocity to have the equilibrium value. Thus, angular disrtibution measurements as the sole means of determining energy exchange are clearly inadequate.

Conclusion

The product angular and translational energy distributions of D_2O have been measured for the temperature range T_s=664-913K. Although the angular distributions can be described by a cosine function, the translational energies are low, <E>/2k=280K at T_s=664K. The low translational energies may be due to non-equilibrium desorption of the D_2O molecule. Assuming this mechanism, the cosine angular distribution and the isotropy of the translational energy imply efficient coupling of tangential and perpendicular motion of the adsorbate. If, however, the final bond formation step and the desorption step are concerted, then the dynamics of the raction are limiting the observed velocities. Features of a dynamical mechanism that could lead to the production of translationally cold molecules are discussed.

Finally, it is becoming increasingly apparent that product molecules do not necessarily thermalize on the surface leading to the loss of the desired dynamical information. These types of measurements are beginning to provide and hold much promise of providing distinctive clues about the potential energy surface for the molecule-surface interaction.

Acknowledgements

This work was supported by the Director, Office of Energy Research, Office of Basic Energy Sciences, Materials Science Division of the U.S. Department of Energy under Contract DE-AC03-76SF00098, and the National Science Foundation. STC gratefully acknowledges the support of Y. T. Lee.

References

1. A.E. Dabiri, T.J. Lee and R.E. Stickney, Surface Sci. 26, 522 (1971).
2. G. Comsa, R. David and K.D. Rendulic, Phys. Rev. Lett. 38, 775 (1977).
3. G. Comsa, R. David and B.-J. Schumacher, Surface Sci. 85, 45 (1979).
4. G. Comsa, R. David, and B.-J. Schumacher, Surface Sci. 95, L210 (1980).
5. C.A. Becker, J.P. Cowin, L. Wharton and D.J. Auerbach, J. Chem. Phys. 67, 3394 (1977).
6. D.A. Mantell, S.B. Ryali, B.L. Halpern, G.L. Haller and J.B. Fenn, Chem. Phys. Lett. 81, 185 (1981).
7. S.L. Bernasek and S.R. Leone, Chem. Phys. Lett. 84, 401 (1981).
8. S.T. Ceyer, Ph.D. Thesis, U. California, Berkeley, 1979.
9. J.N. Smith, Jr. and R.L. Palmer, J. Chem. Phys. 56, 13 (1972)
10. S.T. Ceyer, W.J. Siekhaus and G.A. Somorjai, J. Vac. Sci. Technol. 19, 726 (1981).
11. G. Comsa, R. David and B.-J. Schumacher, Rev. Sci. Instrum. 52, 789 (1982).
12. J.L. Gland, Surfce Sci. 93, 487 (1980)
13. G. Comsa, Proceedings of the Seventh International Vacuum Conference and Third International Conference on Solid Surfaces, 1317 (1977).
14. D.L. Smith and R.P. Merrill, J. Chem. Phys. 53, 3588 (1970).
15. M. Salmeron, R.J. Gale, and G.A. Somorjai, J. Chem. Phys. 67, 5324 (1977) and J. Chem. Phys. 70, 2807 (1979).
16. K. Christmann, G. Ertl, and T. Pignet, Surface Sci. 54, 365 (1976).
17. H. Hopster, H. Ibach, and G. Comsa, J. Catalysis 46, 37 (1977).
18. D.R. Monroe and R.P Merrill, J. Catalysis 65, 461 (1980).
19. H.P. Bonzel and R. Ku, Surface Sci. 40, 85 (1973).
20. B. Lang, R.W. Joyner and G.A. Somorjai, Surface Sci. 30, 454 (1972).

21. W.H. Weinberg, R.M. Lambert, C.M. Comrie and J.W. Linnett, Surface Sci. 30, 299 (1972).

22. K.E. Lu and R.R. Rye, Surface Sci. 45, 677 (1974) and J. Vac. Sci. Technol. 12, 334 (1975).

23. J.L. Gland, B.A. Sexton and G.B. Fisher, Surface Sci. 95, 587 (1980).

24. G.B. Fisher and B.A. Sexton, Phys. Rev. Lett. 44, 683 (1980).

25. L.D. Talley, D.E. Tevault and M.C. Lin, Chem. Phys. Lett. 66, 584 (1979). D.E. Tevault, L.D. Talley and M.C. Lin, J. Chem. Phys. 72, 3314 (1980). L.D. Talley, W.A. Sanders, D.J. Bogan, and M.C. Lin, J. Chem Phys. 75, 3107 (1981).

26. G.B. Fisher and J.L. Gland, Surface Sci. 94, 446 (1980).

27. G. Armand, Surface Sci. 66, 321 (1977).

28. A.T. Modak and P.J. Pagni, J. Chem. Phys. 65, 1327 (1976).

29. J.C. Tully, Surface Sci. 111, 461 (1981).

30. P.J. Pagni and J.C. Keck, J. Chem. Phys. 58, 1162 (1973).

31. E.K. Grimmelmann, J.C. Tully and E. Helfand, J. Chem. Phys. 74, 5300 (1981).

32. H.A. Kramers, Physica 7, 284 (1940).

33. I. Prigogine and E. Xhrouet, Physica 15, 913 (1949).

34. E.W. Montroll and K.E. Schuler, Advances in Chemical Physics 1, 361 (1958).

35. W.J. Siekhaus, J.A. Schwarz and D.R. Olander, Surface Sci. 33, 445 (1972).

36. G. Herzberg, Spectra of Diatomic Molecules (D. Van Nostrand Company, Inc., Princeton N.J., 1950) and Electronic Spectra of Polyatomic Molecules (D. Van Nostrand Company, Inc., Princeton N.J., 1966)

Table I

Temperature, Angle	Translational Energy $\langle E\rangle/2k$	Distribution Width $\langle v^2-\langle v^2\rangle\rangle/\langle v^2\rangle$
664 K, 7°	283 K ± 11 K	0.065 ± 0.013
664 K, 40°	277 K ± 11 K	0.067 ± 0.013
765 K, 7°	305 K ± 12 K	0.065 ± 0.013
870 K, 7°	321 K ± 11 K	0.071 ± 0.013
913 K, 7°	400 K ± 53 K	0.101 ± 0.028
913 K, 47°	470 K ± 53 K	0.101 ± 0.029

Figure Captions

1. Schematic diagram of the molecular beam scattering apparatus.
2. TOF distributions of D_2O from a thermal effusive source. The solid line is a Maxwell-Boltzmann distribution at the temprature indicated by the thermocouple. (a) 310K. (b) 655K.
3. Product D_2O angular distributions, $T_s = 700K$. (a) $D_2 + O_2$ (b) $D + O_2$.
4. D_2O translational energy distributions for (a) $T_s = 913K$, $\Theta = 7°$ (b) $T_s = 870K$, $\Theta = 7°$ (c) $T_s = 765K$, $\Theta = 7°$. Open circles represent the corresponding Maxwell-Boltzmann distributions.
5. D_2O translational energy distributions for $T_s = 664K$ (a) $\Theta = 7°$ (b) $\Theta = 40°$. Open circles represent the corresponding Maxwell-Boltzmann distribution.
6. D_2O production rate on Pt(111) (a) as a function of surface temperature (b) as a function of O_2 source stagnation pressure.
7. Energy levels of reactants, intermediates and products. D binding energy from [22], O binding energy from [12,23], OD binding energy from [25], D_2O binding energy from [26], gas phase bond energies from [36].
8. Diagramatic representation of D_2O desorption. The solid curve is the equilibrium population of energy levels given by the Boltzmann function, exp(-E/R 870K), for energy E, and is drawn relative to the 15 kcal/mole Pt-D_2O well depth [26] (dashed line). The appearance into the gas phase is proportional to v_z [27], and increases with energy above the edge of the potential energy well, as indicated by the arrows. Molecules are excited to the higher energy states by thermal excitation.
9. Mean D_2O translational energy versus the mean energy expected for equilibrium at the surface temperature.

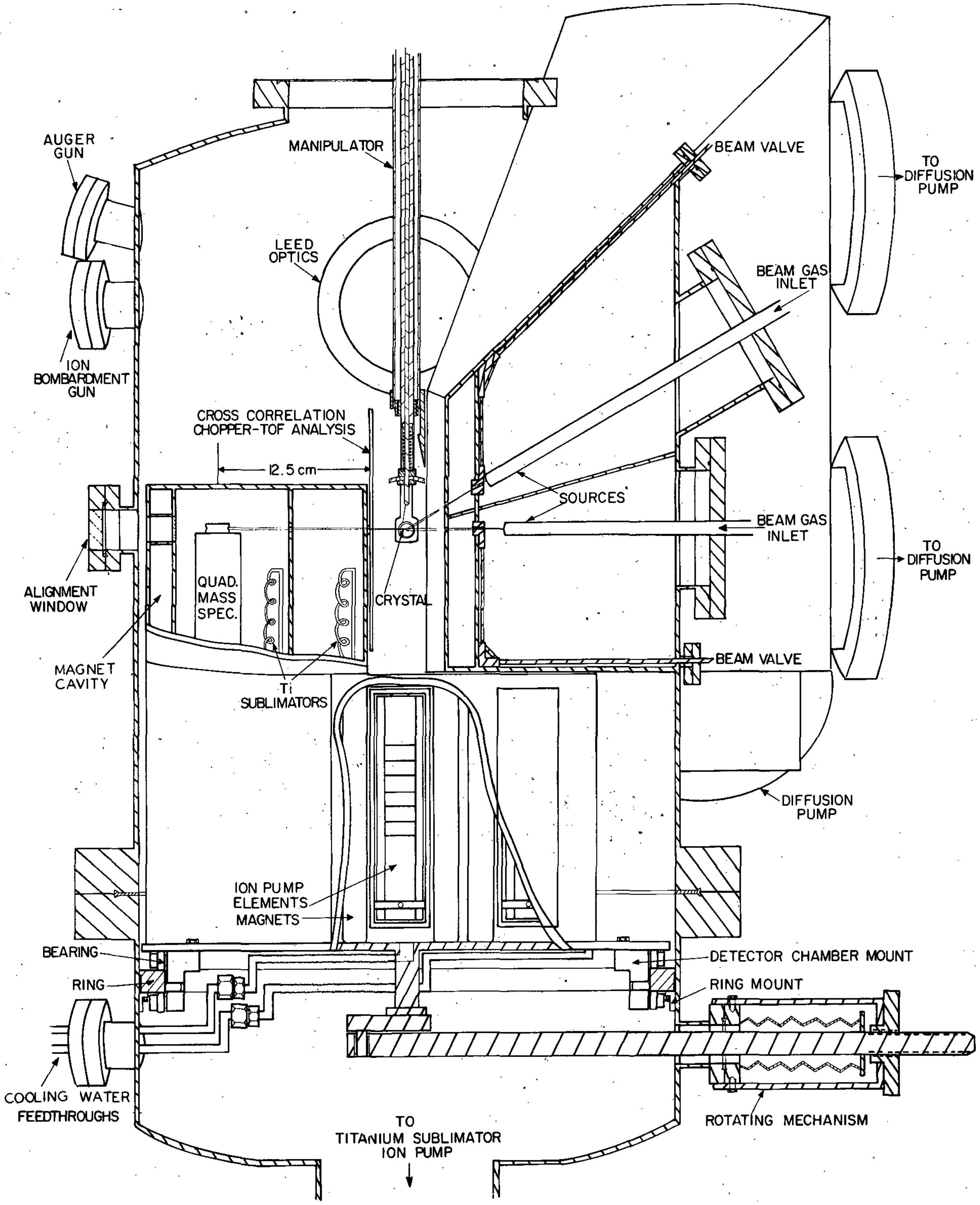

XBL 799-11376

Fig. 1

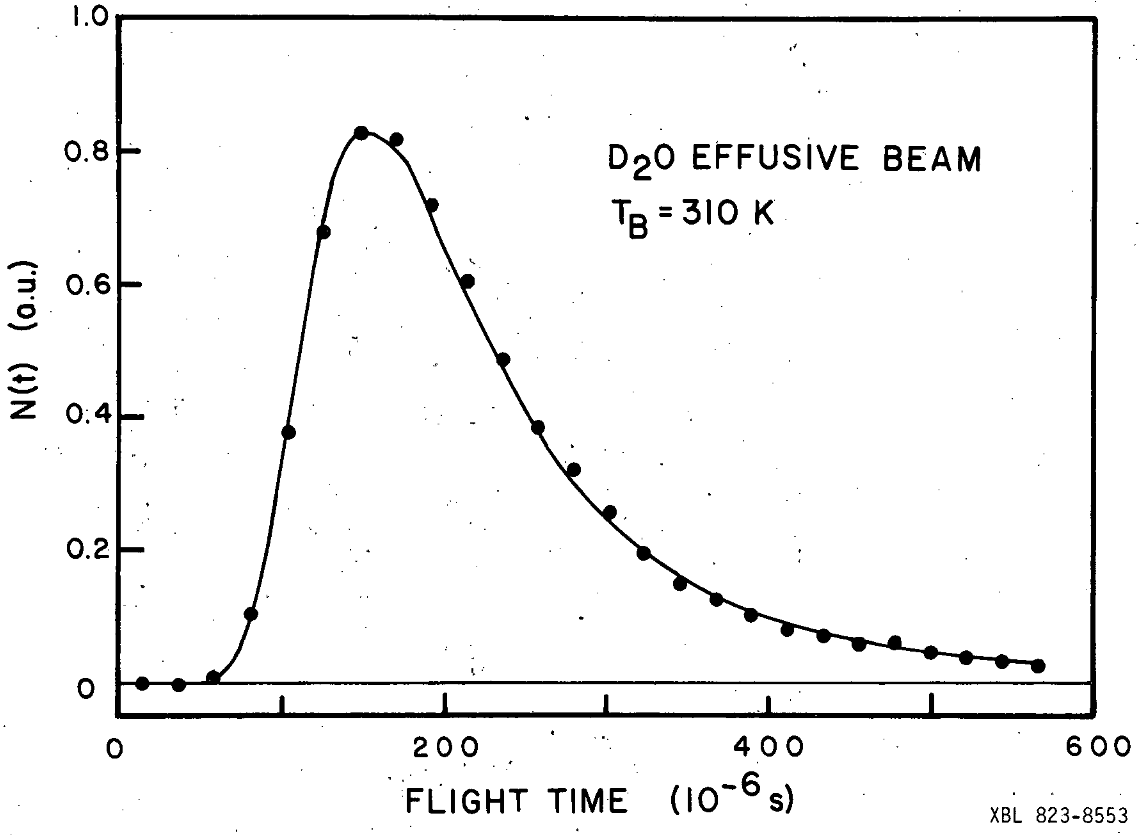
1.0
0.8
0.6
0.4
0.2
0
N(t) (a.u.)
0
200
400
600
FLIGHT TIME (10^{-6} s)
D_2O EFFUSIVE BEAM
T_B = 310 K
XBL 823-8553

Fig. 2a

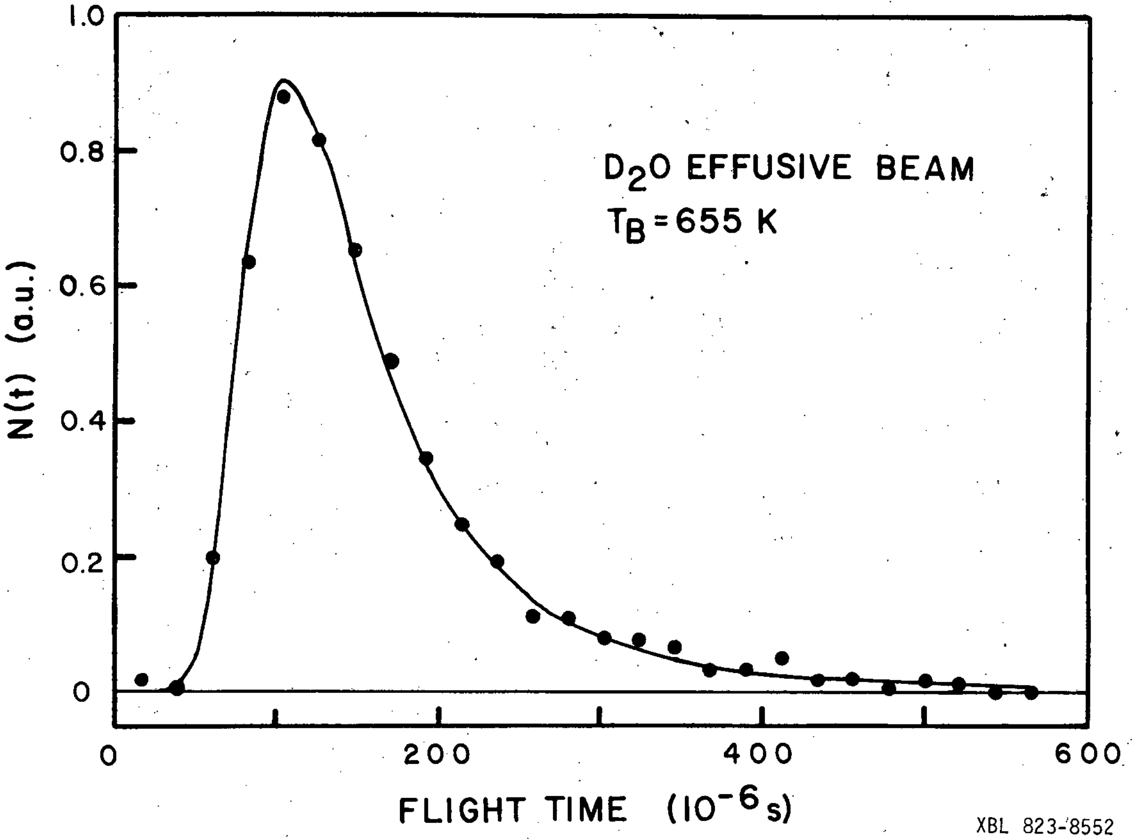

XBL 823-8552

Fig. 2b

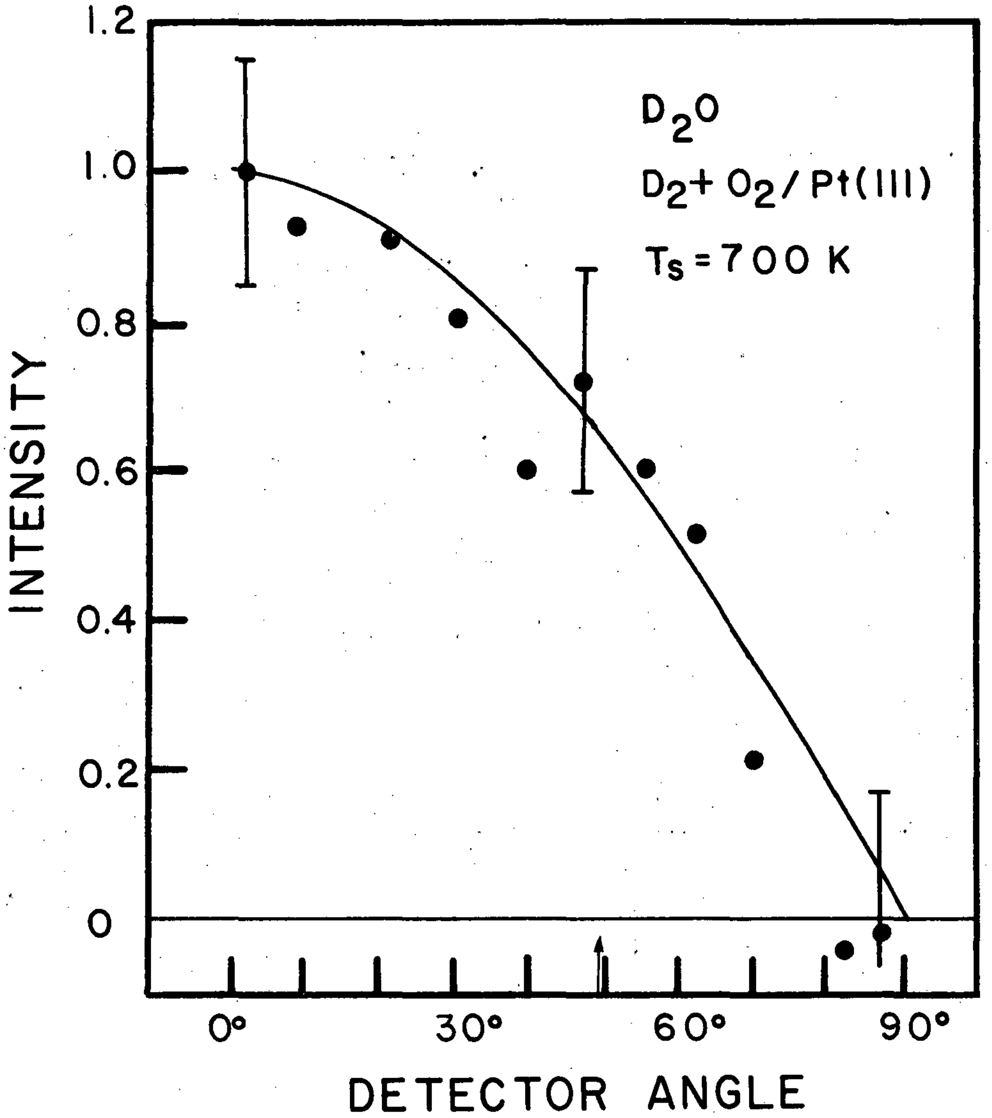

XBL 823-8551

Fig. 3a

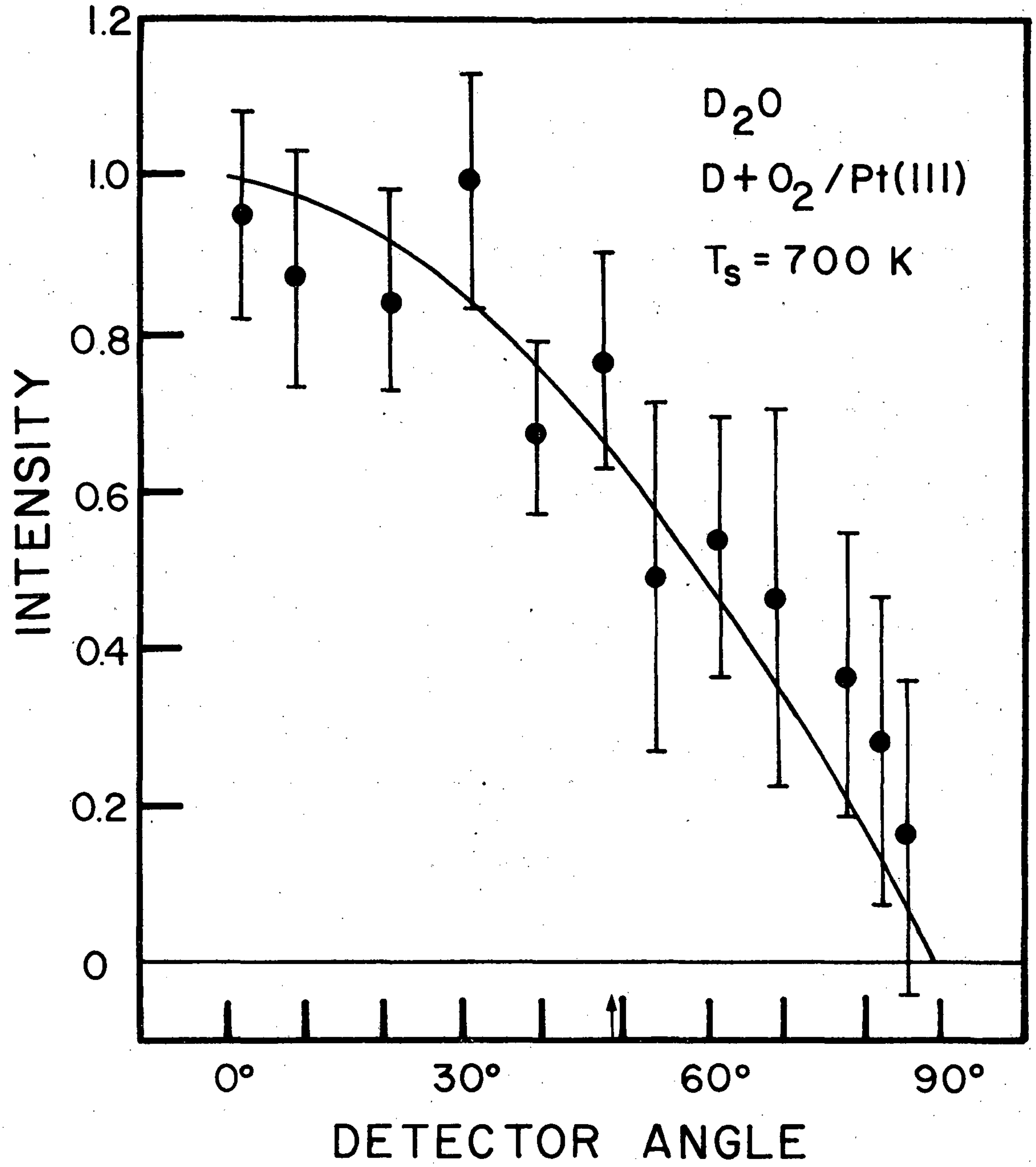

XBL 828-9595

Fig. 3b

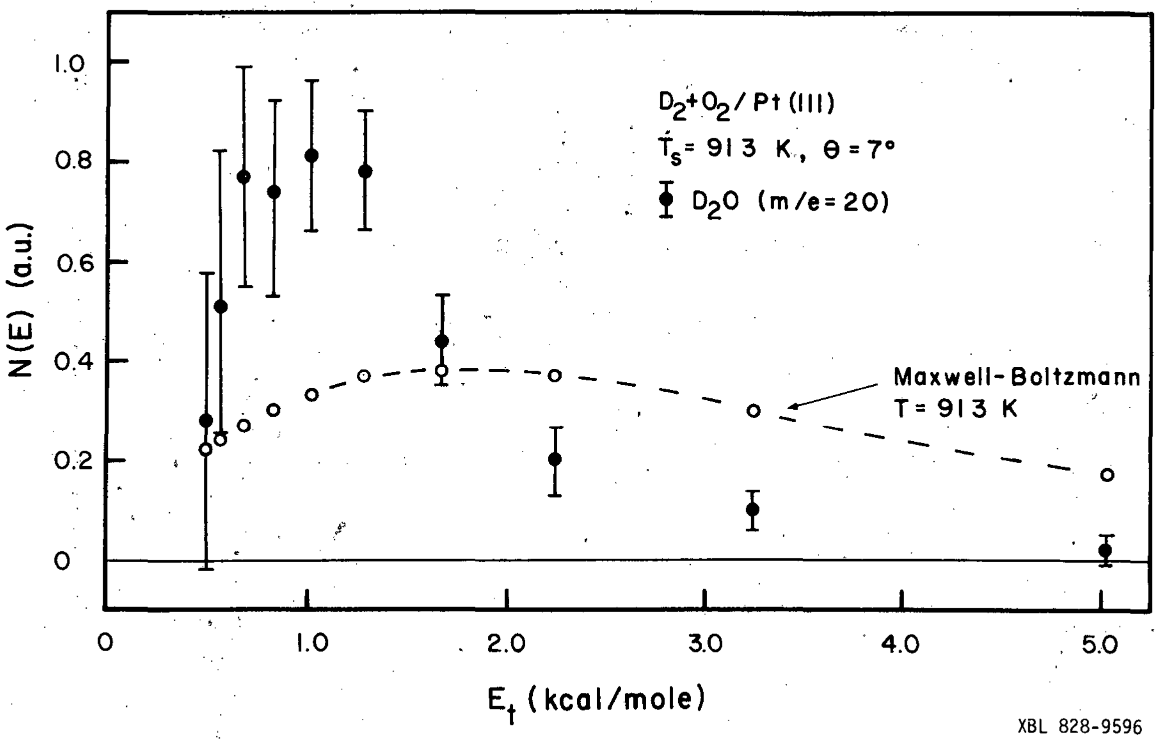

1.0
0.8
0.6
0.4
0.2
0
N(E) (a.u.)
D_2+O_2/Pt(111)
T_s= 913 K, θ = 7°
● D_2O (m/e=20)
Maxwell-Boltzmann
T= 913 K
0
1.0
2.0
3.0
4.0
5.0
E_t (kcal/mole)
XBL 828-9596

Fig. 4a

Fig. 4b

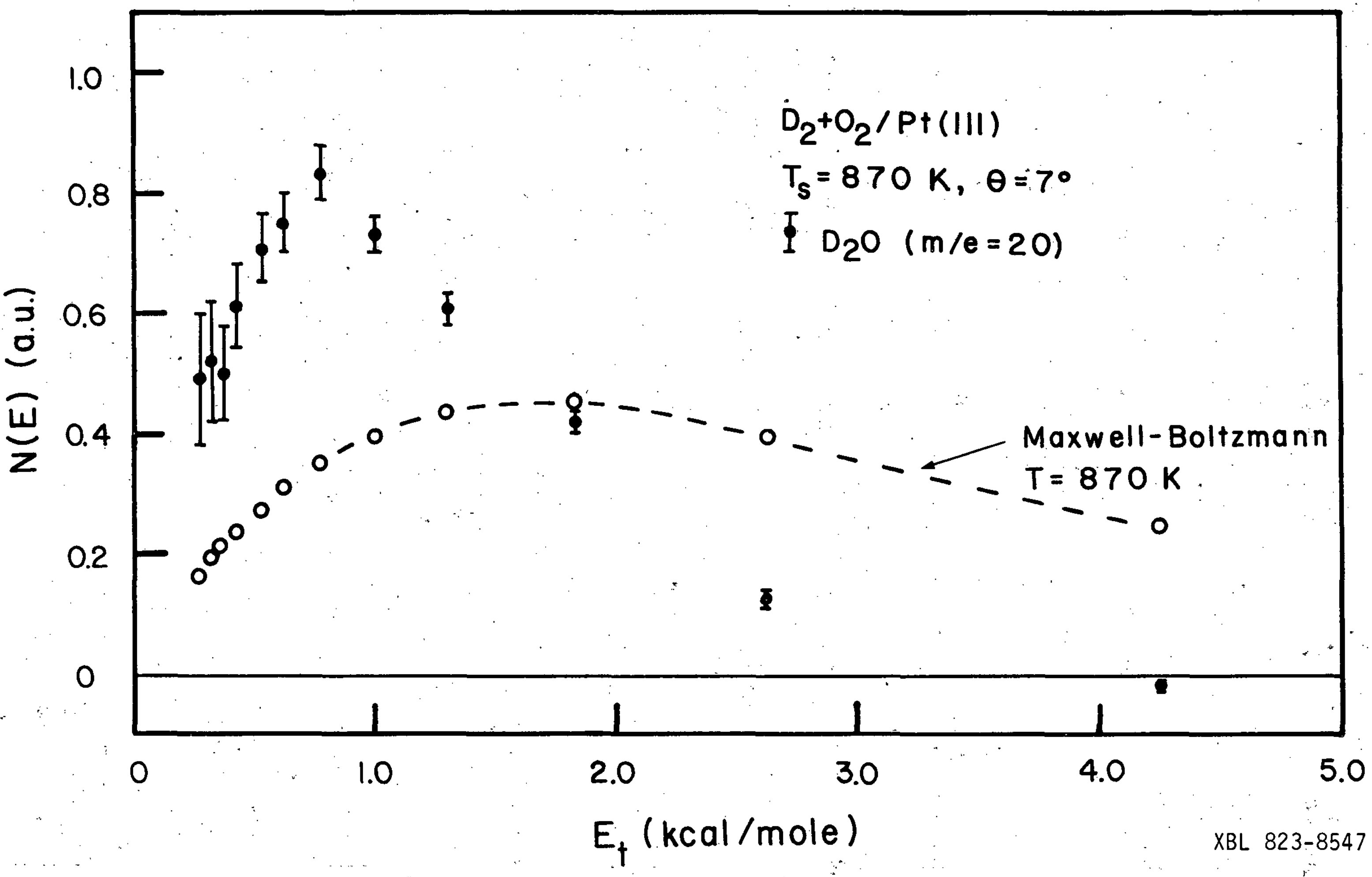

XBL 823-8547

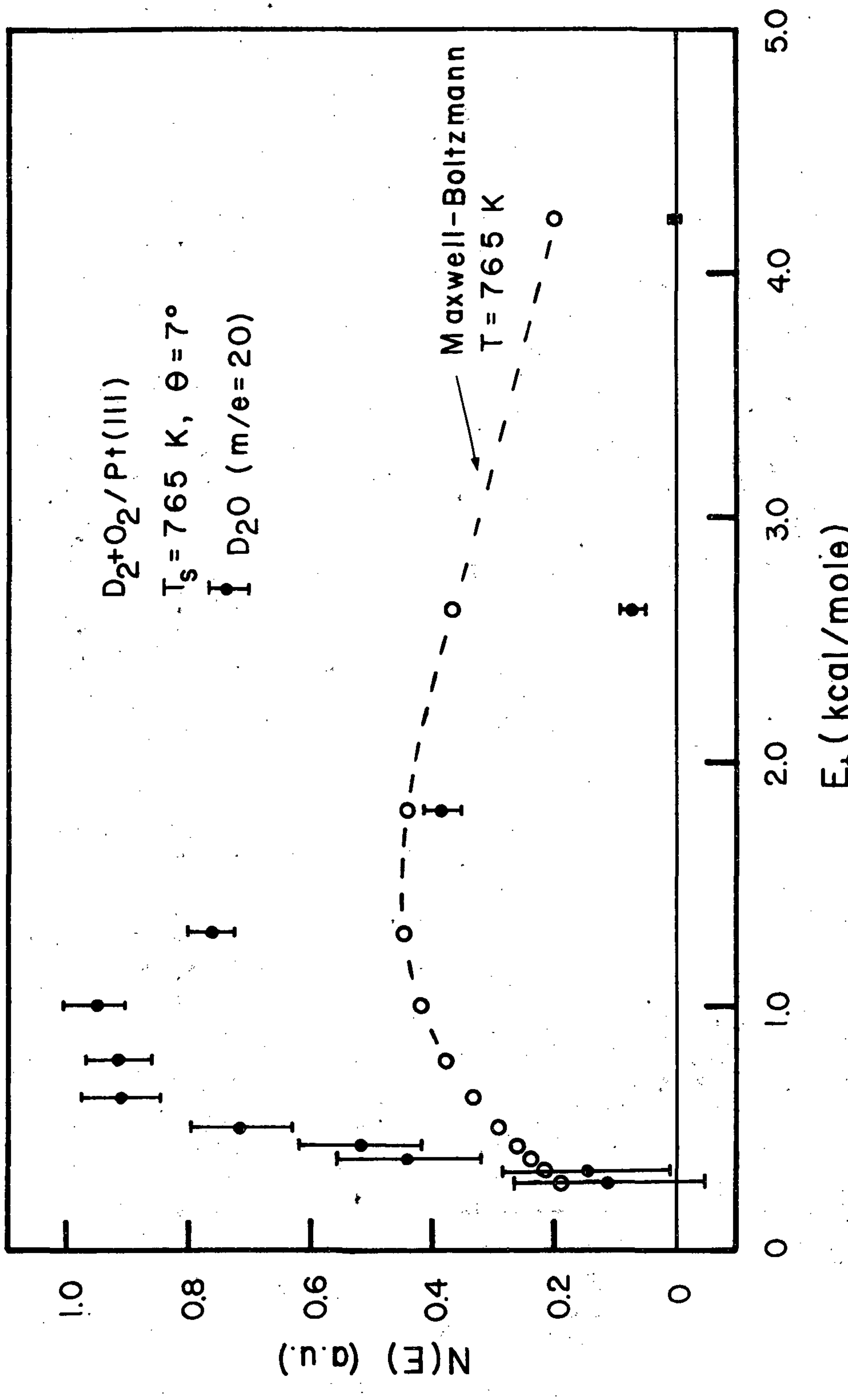

XBL 823-8548

Fig. 4c

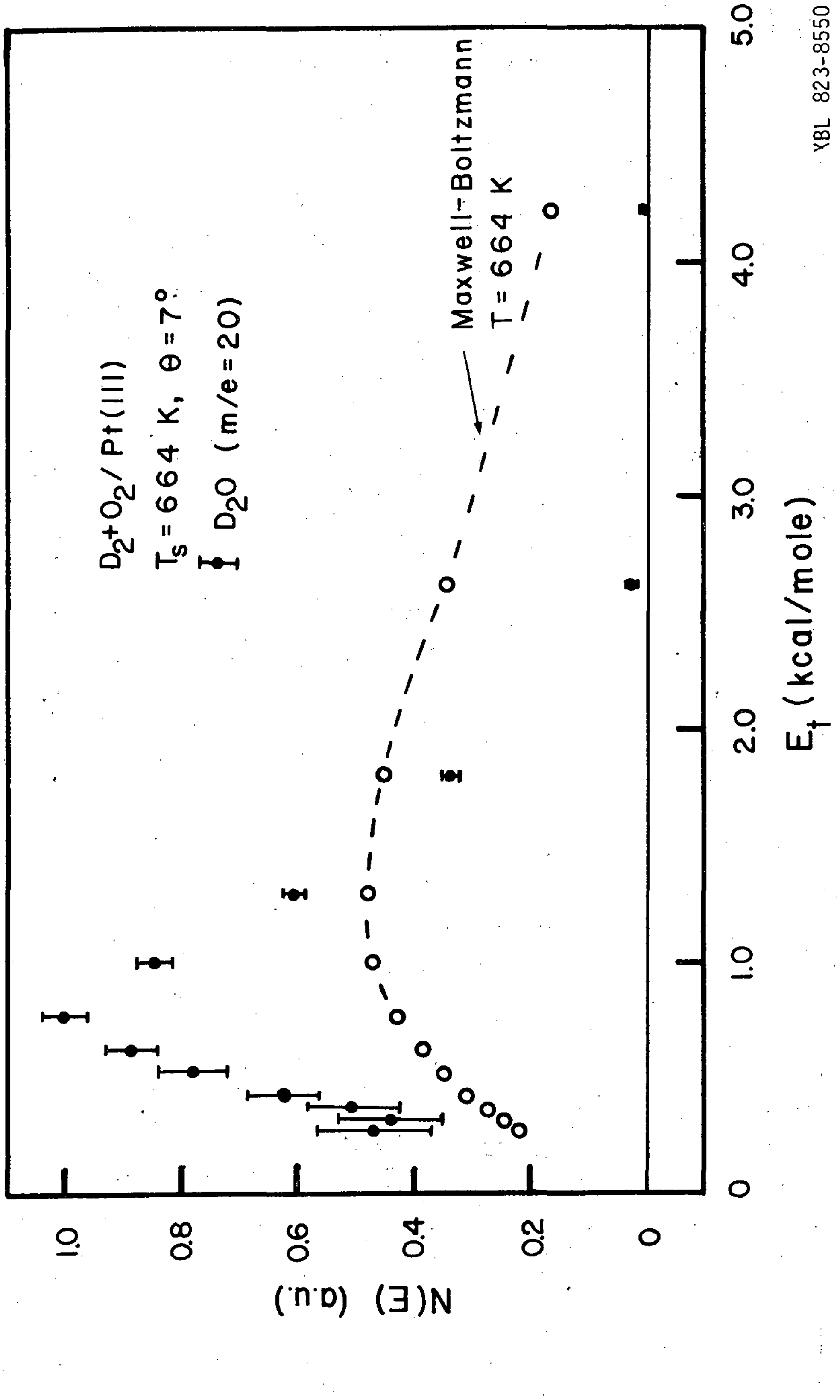
D2+O2/Pt(111)
Ts = 664 K, θ = 7°
D2O (m/e = 20)
Maxwell-Boltzmann
T = 664 K
N(E) (a.u.)
1.0
0.8
0.6
0.4
0.2
0
Et (kcal/mole)
0
1.0
2.0
3.0
4.0
5.0
YBL 823-8550

Fig. 5a

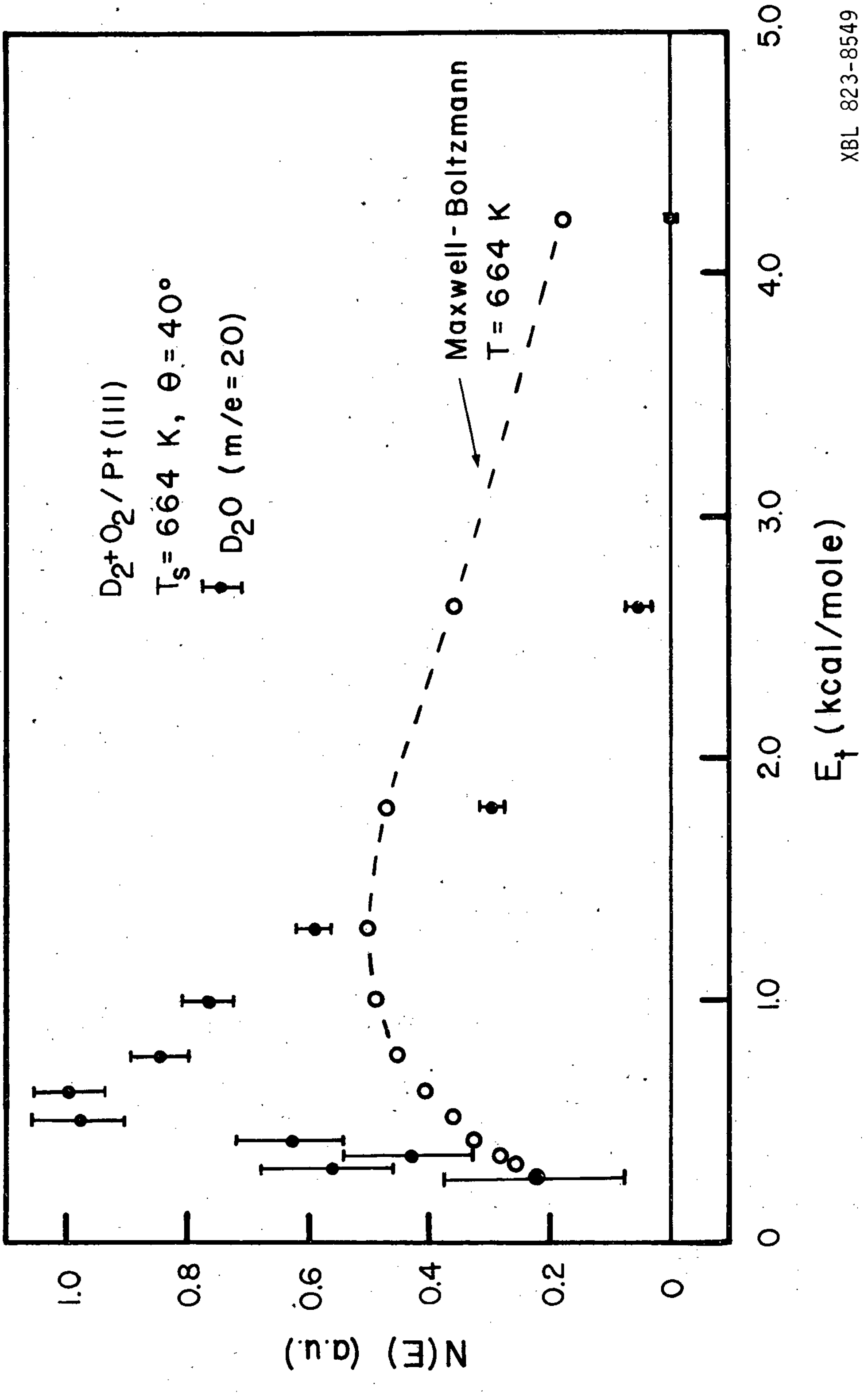

XBL 823-8549

Fig. 5b

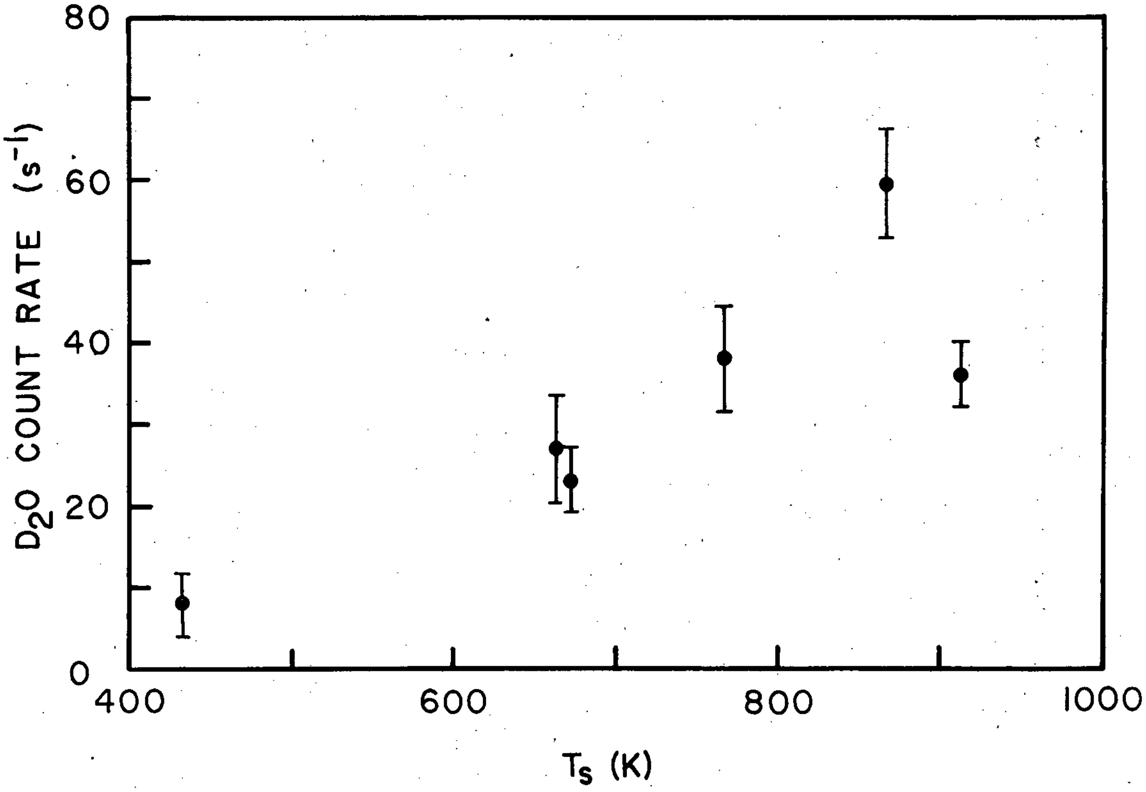

XBL 828-9597

Fig. 6a

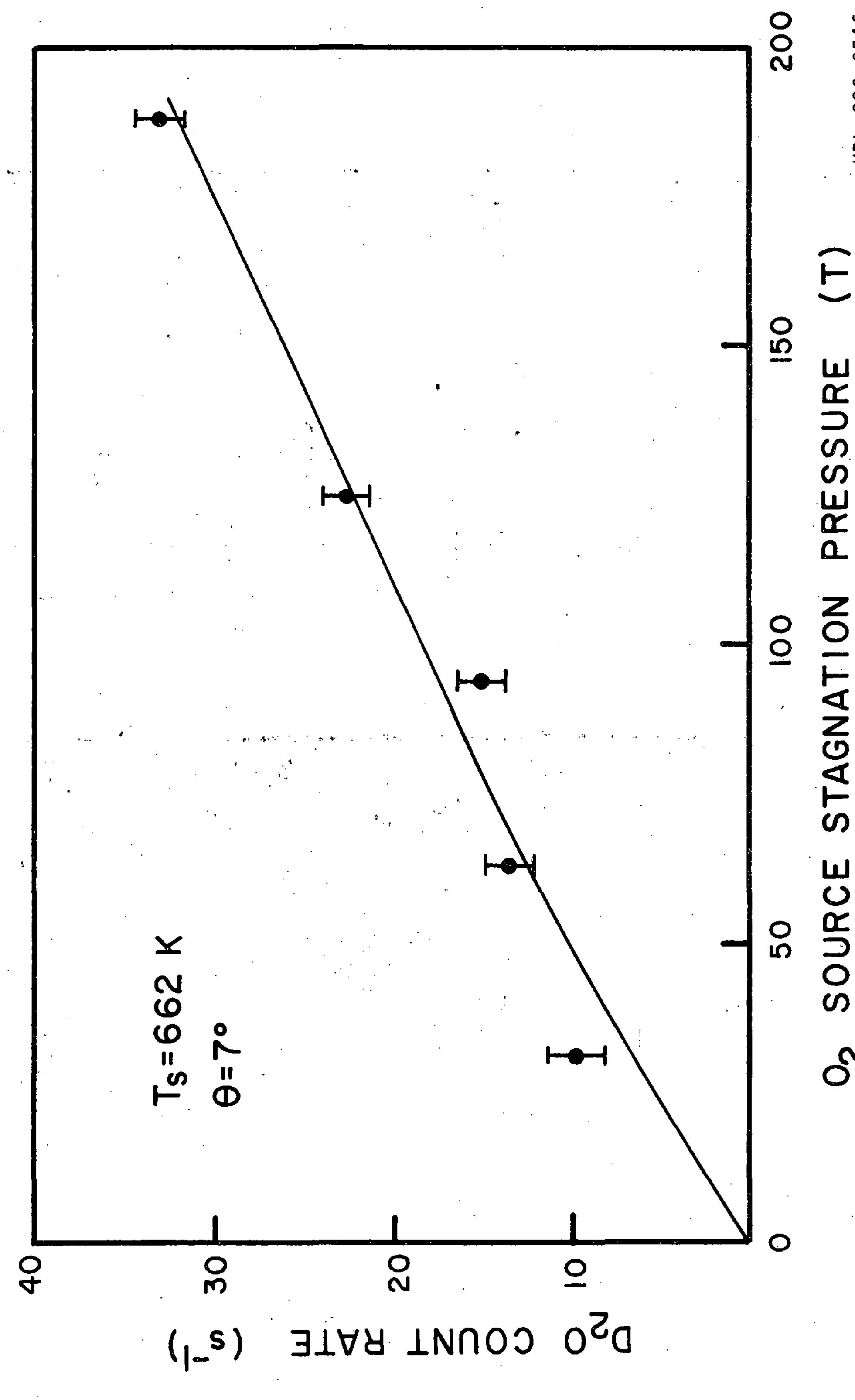

XBL 823-8546

Fig. 6b

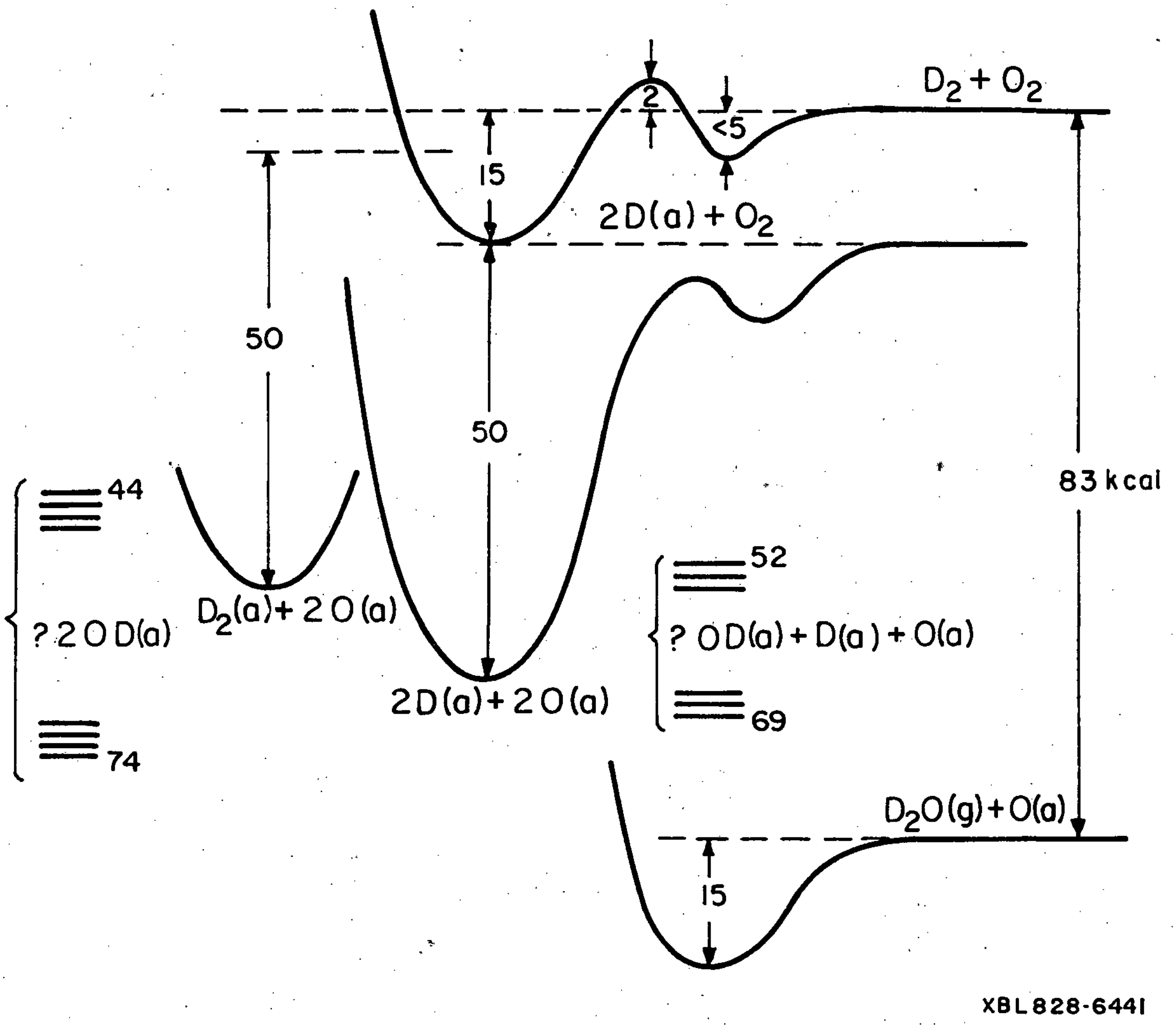
D$_2$ + O$_2$
2
<5
15
2D(a) + O$_2$
50
50
83 kcal
44
?2OD(a)
74
D$_2$(a)+2O(a)
2D(a)+2O(a)
52
?OD(a)+D(a)+O(a)
69
D$_2$O(g)+O(a)
15
XBL 828-6441

Fig. 7

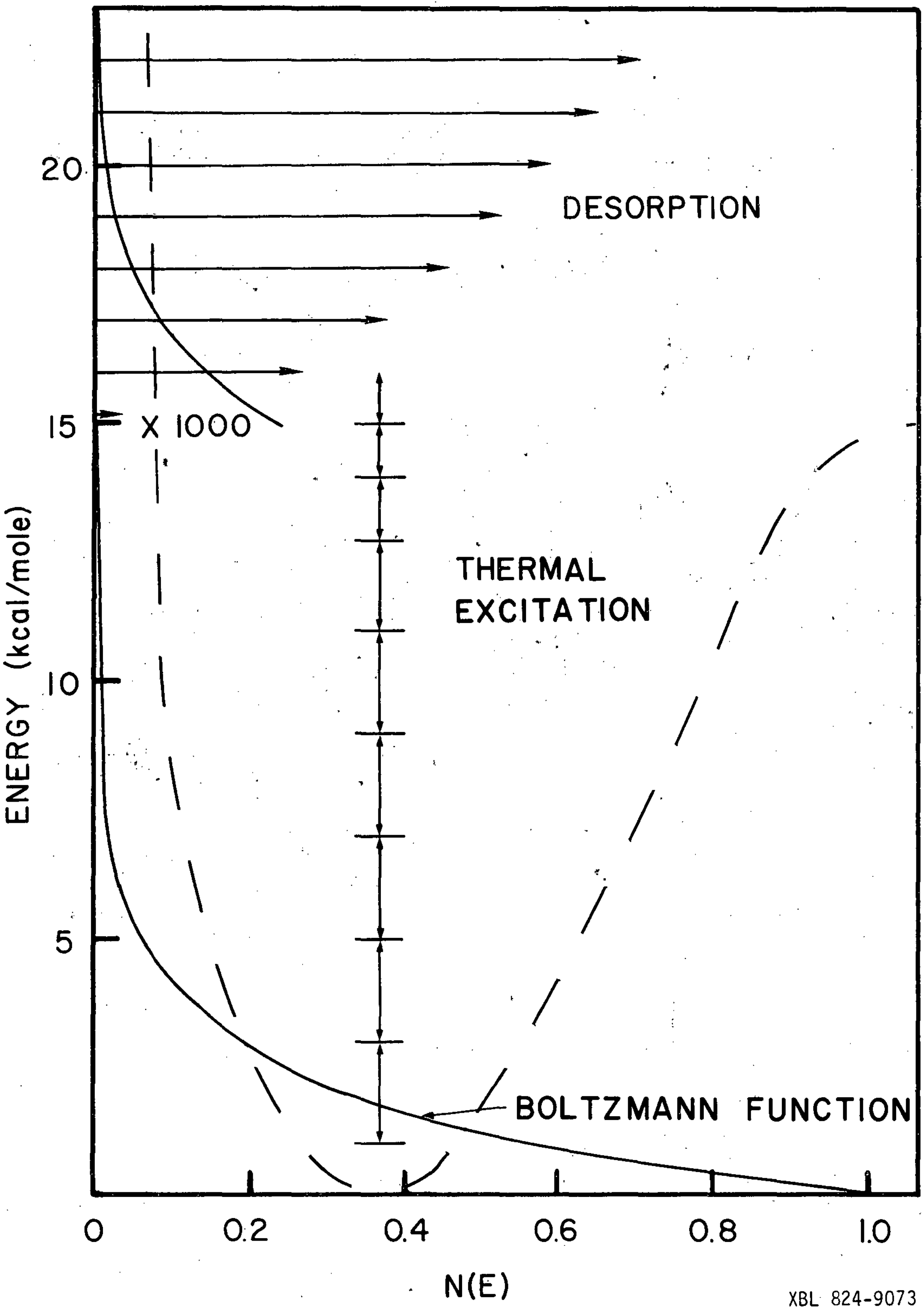
DESORPTION
THERMAL
EXCITATION
BOLTZMANN FUNCTION
X 1000
ENERGY (kcal/mole)
20
15
10
5
0
0.2
0.4
0.6
0.8
1.0
N(E)
XBL 824-9073

Fig. 8

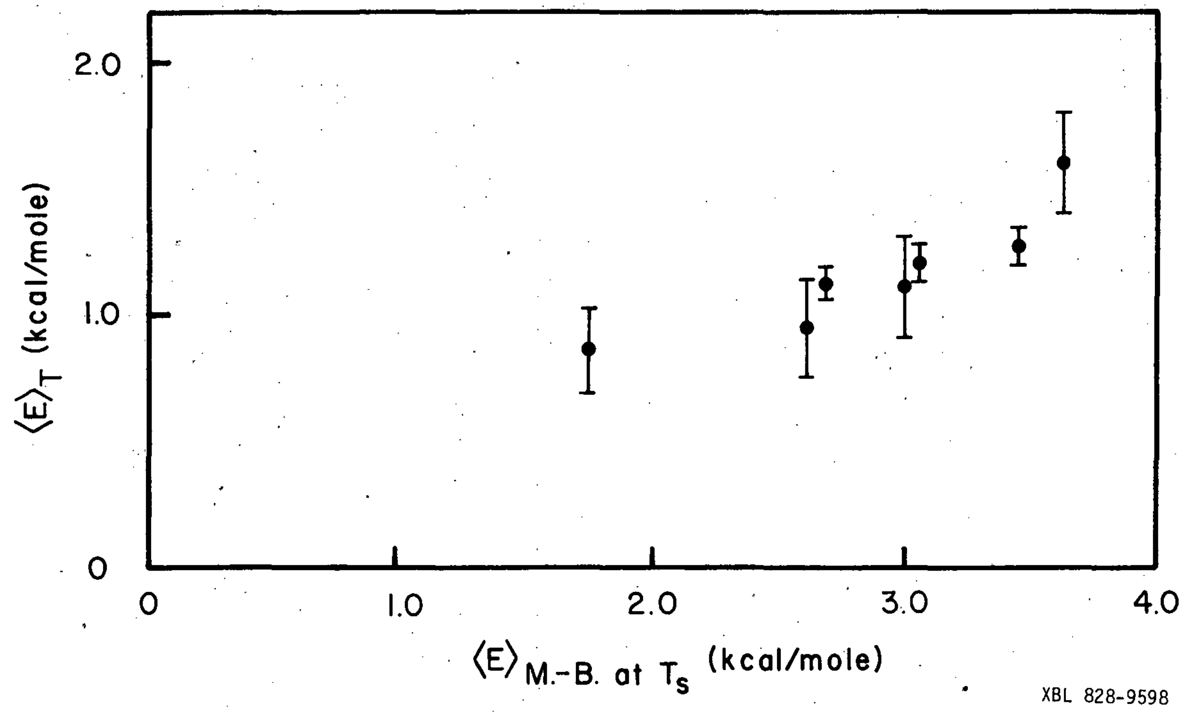
2.0
1.0
0
0
1.0
2.0
3.0
4.0
$\langle E \rangle_T$ (kcal/mole)
$\langle E \rangle_{M.-B.\ at\ T_s}$ (kcal/mole)
XBL 828-9598

Fig. 9

TECHNICAL INFORMATION DEPARTMENT
LAWRENCE BERKELEY LABORATORY
UNIVERSITY OF CALIFORNIA
BERKELEY, CALIFORNIA 94720